



## Derivation of mathematical expressions to define resonant ejection from square and sinusoidal wave ion traps

Hideya Koizumi<sup>a</sup>, William B. Whitten<sup>a</sup>, Peter T.A. Reilly<sup>a,\*</sup>, Eiko Koizumi<sup>b</sup>

<sup>a</sup> Oak Ridge National Laboratory, Oak Ridge, TN 37831, United States

<sup>b</sup> Department of Mathematics, Peace College, Raleigh, NC 27604, United States

### ARTICLE INFO

#### Article history:

Received 11 May 2009

Received in revised form 17 June 2009

Accepted 19 June 2009

Available online 27 June 2009

#### Keywords:

Ion trap mass spectrometry

Resonance ejection

Digital ion trap

Sinusoidal ion trap

### ABSTRACT

Resonant ejection for mass analysis with ion traps is widely used because it markedly improves the mass range and resolution of ion traps. Unfortunately, an easy-to-use analytical expression that defines the ejection mass as a function of the trapping and excitation frequencies is missing in the literature because the secular frequency of the ions in sinusoidal ion traps is not easily determined for all stable values of  $q_z$  from the Mathieu equation. However, the ion secular frequency for all stable values of  $q_z$  in digital ion traps can be readily determined from Hill's equation. We have taken this expression and solved it for  $q_z$  to produce an analytical expression for the ejection mass as a function of trapping and excitation frequency. We also recognized that the expression for the ion mass during resonant ejection for a square wave driven trap can be converted to an expression for a sinusoidal wave trap merely by multiplication by a factor of  $4/\pi$ . These new expressions open up the possibility of rapid mass calibration for any method of resonant ejection from square or sinusoidal wave driven ion traps.

© 2009 Elsevier B.V. All rights reserved.

### 1. Introduction

Since the ion trap was introduced, it has become a major analytical tool whose utility seems to be increasing by the day. One of the most recent advances in ion trap technology is the digital ion trap mass spectrometer [1–3]. Richards et al. [4,5] were the first to experimentally verify the feasibility of using rectangular waveforms with quadrupole mass filters. However, Ding et al. [1–3] were the first to digitally produce square waves, amplify them with high voltage DC pulsers and step the square wave frequency rapidly to produce a digital ion trap mass spectrum. The digital ion trap has not yet been exploited as a commercial product, but we guess that it soon will. Current commercial ion traps operate with sinusoidal potentials and are called SITs in this publication. Ion traps that operate with digitally produced square wave potentials are called DITs. SITs generally perform mass scans by linearly varying the voltage of the trapping potential waveform. DITs, on the other hand, generally perform mass scans by stepping the frequency of the applied potentials.

It is the ability to precisely produce and rapidly step the applied waveforms that make DITs so unique. Low voltage digital waveforms are produced by direct digital synthesis (DDS) [6,7]. The

high voltage waveform applied to the ring electrode is produced by amplifying the digital waveforms with a high voltage pulser circuit. DDS technology can produce waveforms with up to 48-bit frequency stepping resolution ( $2^{48} \approx 3 \times 10^{14}$ ) [8]. Of course, this resolution will never manifest itself because of all the other uncertainties associated with producing waveforms; however, it does point toward the potential of the technique. It also means that the frequency control is so precise that the mass can be stepped linearly during a frequency sweep if you precisely know how the mass of the ejected ion changes with the frequency of the applied potentials.

SITs and DITs have two basic operational modes, mass instability and resonance ejection. In the mass instability mode, ejection occurs when the ion crosses the boundary of stability ( $\beta_z = 1$ ) imposed by the ring potential. Resonance ejection occurs by the application of an auxiliary potential, generally applied across the endcap electrodes. When the frequency of the auxiliary or excitation waveform,  $f_{\text{aux}}$ , matches the frequency of ion oscillation in the trap, the ion is resonantly ejected. Locked resonant ejection occurs by constraining the frequency of the auxiliary potential to values that are defined by the frequency of the ring potential divided by an integer ( $f_{\text{aux}} = f_{\text{ring}}/n$ , where  $n \geq 3$ ). The normal operation of a DIT varies the frequency while holding the amplitude of the square waveform constant. Conversely, the normal operation mode of a SIT holds the frequency of the sinusoidal waveform constant while varying the amplitude.

\* Corresponding author at: Oak Ridge National Laboratory, PO Box 2008, MS 6142, Oak Ridge, TN 37831, United States. Fax: +1 865 574 8363.

E-mail address: [ReillyPT@ornl.gov](mailto:ReillyPT@ornl.gov) (P.T.A. Reilly).

During a resonant ejection scan in a SIT with fixed excitation waveform, the ejected mass varies linearly with the voltage of the waveform. Therefore, the mass can be easily calibrated with standards. In DITs, the ejected mass is only directly proportional to  $\Omega^{-2}$  when the trapping and excitation frequencies are phase locked. This makes calibration more difficult when the system is not phase locked. Georinger et al. [9] produced excellent resolution (45,000) when they held the trapping potential of a SIT constant and very slowly swept the excitation frequency. This technique never gained popularity, in part, because the mass is not easily correlated with the excitation frequency over a wide range and it is more difficult to mass calibrate the system.

Consequently, expressions defining the ejection mass as a function of any trapping and excitation waveform are needed to help further develop resonance ejection in SITs and DITs. In this paper, we provide the derivation of these expressions for ejection mass as a function of any combination of trapping and excitation waveform frequencies in SITs and DITs. Providing these expressions will enhance the range of possibilities for mass analysis with ion traps especially considering the advances in the direct digital synthesis of waveforms.

## 2. Derivation of expressions for resonant ejection from SITs and DITs

The Mathieu equations [10,11] completely describe the motion of ions due to a sinusoidal trapping potential waveform at  $0 \leq q_z \leq 0.908$ . The motion of the trapped ions can be described by a low frequency (secular) oscillation imposed upon a high frequency ripple. At higher values of  $q_z$  ( $q_z > 0.4$ ), the high frequency oscillations increase in amplitude and a beat pattern is formed [12]. Resonant ejection is produced with the application of an auxiliary potential between the endcap electrodes. When the frequency of the secular motion and the applied auxiliary potential match, the ion is resonantly ejected from the trap. The key to defining the conditions for resonant ejection from the trap is the definition of the secular frequency of the ions.

Dehmelt [13] employed what is now known as the pseudo-potential well model to help define the ion's secular motion. This model neglects the high-frequency ripple and assumes that the motion of the ion along a coordinate can be approximated by an ion undergoing simple harmonic motion in a parabolic potential well. This treatment defines the secular frequency,  $\omega_{\text{sec}}$ , as a function of the Mathieu parameter,  $q_z$  and the radial trapping frequency,  $\Omega$ , in the following expression:

$$\omega_{\text{sec}} = \frac{q_z \Omega}{2\sqrt{2}} \quad (1)$$

In SITs, values of  $q_z$  between 0 and 0.908 yield stable ion trajectories. However, the linear relation between  $q_z$  and  $\omega_{\text{sec}}$  is valid only below  $q_z = 0.4$ . Trevitt et al. [14] produced a better approximation of the ion secular frequency in a SIT with the following formula:

$$\omega_{\text{sec}} = \left( \frac{q_z^2}{2 - q_z^2} - \frac{7}{128} q_z^4 + \frac{29}{2304} q_z^6 \right)^{1/2} \frac{\Omega}{2} \quad (2)$$

The derivation of this expression can be found in McLachlan's text on Mathieu functions [15]. This approximation restricts the values of  $q_z$  to be less than 0.7. Both approximations assume there is no net DC potential between the ring and endcap electrodes. It would be useful to have an expression for the secular frequency of ions for any stable value of  $q_z$ . Unfortunately, an analytical expression relating  $q_z$  and  $\omega_{\text{sec}}$  cannot easily be derived directly from the Mathieu equation.

For digital ion traps, ion motions are determined by the applied periodic square wave potentials described by Hill's equation. Ding

et al. [2] used matrix methods to derive an exact expression for  $\beta_z$  that easily yielded the following expression for  $\omega_{\text{sec}}$ :

$$\omega_{\text{sec}} = \frac{\beta_z \Omega}{2} = \frac{\Omega}{2\pi} \arccos \left( \cos \left( \pi \sqrt{\frac{q_z}{2}} \right) \cosh \left( \pi \sqrt{\frac{q_z}{2}} \right) \right) \quad (3)$$

This expression is valid for all stable values of  $q_z$ . Our goal here is to derive an expression for the mass of the ion resonantly ejected from the trap at any applied trapping and excitation frequency. Therefore, an expression for  $q_z$  as a function of  $\omega_{\text{sec}}$  is required. Solving Eq. (3) for  $q_z$  requires expanding the cos and cosh functions in Taylor series:

$$\cos \pi \beta_z = \cos \left( \pi \sqrt{\frac{q_z}{2}} \right) \cosh \left( \pi \sqrt{\frac{q_z}{2}} \right) = \left[ \sum_{n=0}^{\infty} \frac{(-1)^n}{(2n)!} x^{2n} \right] \times \left[ \sum_{n=0}^{\infty} \frac{x^{2n}}{(2n)!} \right] \quad (4)$$

where  $x = \pi(q_z/2)^{1/2}$ . The expansions were carried out to the  $n=4$  term and like terms were collected. The odd  $n$  terms canceled and the expansion product was truncated at the  $x^8$  term yielding the following quadratic equation:

$$0 = 1 - \cos \pi \beta_z - \frac{x^4}{6} + \frac{x^8}{2520} \quad (5)$$

Applying the restrictions given by mass instability and ignoring the imaginary solutions yields a single analytical equation for  $q_z$  as a function of  $\Omega$  and  $\omega_{\text{ex}}$

$$q_z = \frac{4}{\pi^2} \left\{ \frac{3}{2} \left[ 35 - \sqrt{1225 - 70 \left( 1 - \cos \left( \frac{2\pi\omega_{\text{ex}}}{\Omega} \right) \right)} \right] \right\}^{1/2} \quad (6)$$

The validity of the equation can be checked by setting  $2\omega_{\text{ex}} = \Omega$ . We obtained the calculated value of  $q_z = 0.7125$  correctly corresponding to the value of  $q_z$  at the stability boundary for a DIT. Similarly, the values of  $q_z$  for frequency locked resonance ejection can be obtained using the relation  $1/n = \omega_{\text{ex}}/\Omega$  where  $n$  is an integer number greater than or equal to 3. This will reproduce the table of ejection  $q_z$  values for phase locked operation found in Ding et al. [2]. Further validation of our equation was obtained by plotting Ding et al.'s simulation data [3] of the ion secular frequency as a function of  $q_z$  for a trapping frequency of 500 kHz. In Fig. 1, we have reproduced Fig. 5 from Ding et al.'s manuscript [3] and overlaid the plot of our equation. The circles represent their data and the dashed line represents the pseudo-potential approximation (Eq. 1) [1]. The result of our equation is plotted as a solid line. It overlays the line they (and we) found using Eq. (3) [3].

Given the fact the Ding et al.'s expression is exact and ours is an approximation that results from truncation of the expansion, the overlap of the expressions was better than expected. We wanted to know how good our approximation was. We then used Ding et al.'s expression (Eq. (3)) to calculate  $\omega_{\text{sec}}$  for a range of  $q_z$  spanning the stable values. We used those values in our Eq. (6), under the same conditions, to calculate  $q_z$ . The original values of  $q_z$  were then subtracted from our calculated  $q_z$  and the differences were plotted as a function of  $q_z$  in Fig. 2. At values of  $q_z$  less than 0.5 the difference or error is less than  $1 \times 10^{-5}$ . The maximum difference at  $q_z = 0.7125$  is approximate  $4.5 \times 10^{-5}$ . These differences are in general much less than the typical experimental error in ion trap mass spectrometry. Therefore, our expression for  $q_z$  in a resonant ejection experiment may not be truly exact, but it is a better approximation than most experiments require. We now have a valid expression to calculate the value of  $q_z$  for any ion ejected from a DIT at any value of the trapping and excitation frequency.

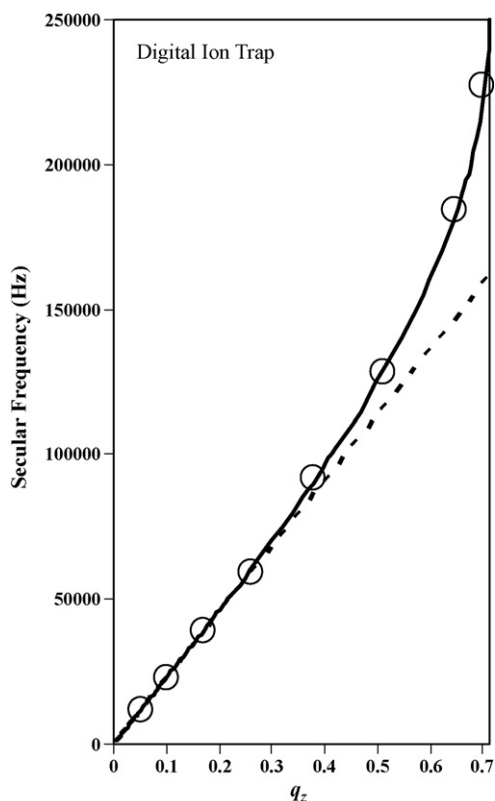


**Fig. 1.** A plot of the ion secular frequency in a DIT operated at a trapping frequency of 500 kHz versus the Mathieu parameter,  $q_z$ , derived from Eq. (6) is shown as a solid black line. A plot of the ion secular frequency using the pseudo-potential well approximation is depicted as a dashed line. The open circles represent the simulation data extracted from Fig. 5 in reference [3]. Our results reproduce the work of Ding et al. [3].

We recognized that the results of our expression for  $q_z$  in DITs should be applicable to SITs because a square wave can be represented as a Fourier expansion of sine waves:

$$f(x) = \frac{4}{\pi} \sum_{n=1}^{\infty} \frac{1}{n} \sin\left(\frac{n\pi x}{L}\right) \quad (7)$$

where  $2L$  is the period of the wave and  $x$  is the frequency. The odd terms are non-zero. Only the first term in the series affects the stability of the ions. The contributions from the higher order components at 3, 5, 7, ... times the frequency affect the time dependence but do not significantly affect the stability of the ions. Consequently, the difference between the ion motion produced by a square wave and that produced by a sine wave is a factor of  $4/\pi$ . The factor of  $4/\pi$  often occurs when comparing sinusoidal and square wave ion traps. For example, the difference between the values of  $q_z$  at the  $\beta = 1$  boundary for SITs and DITs is to an excellent approximation  $4/\pi$ . Therefore, multiplying Eq. (4) by a factor of  $4/\pi$  yields the correct expression for  $q_z$  in a SIT. A direct comparison of the behavior of  $q_z$  with respect to the excitation frequency,  $\omega_{\text{ex}}$ , can be obtained from Eqs. (1) and (2) (see Fig. 3). Our expression is plotted as a solid line. The pseudo-potential well approximation from Eq. (1) is plotted as a dotted line that deviates from our expression near  $q_z = 0.4$ . The expression of Trevitt et al. [14] is plotted as a dashed line. It deviates from our result at  $q_z = 0.7$  where they claimed that their expression breaks down.

It follows that the frequency of any mass under any resonant ejection conditions in a DIT can be found by substituting Eq. (4) into the relationship between the ion mass,  $m$  and the Mathieu

parameter,  $q_z$

$$m_{\text{ej}} = \frac{8eV}{q_z \bar{r}_0^2 \Omega^2} = \frac{2\pi^2 eV}{\bar{r}_0^2 \Omega^2} \left\{ \frac{3}{2} \left[ 35 - \sqrt{1225 - 70 \left( 1 - \cos\left(\frac{2\pi\omega_{\text{ex}}}{\Omega}\right)\right)} \right] \right\}^{-1/2} \quad (8)$$

$V$  is the trapping potential amplitude,  $e$  is the electron's charge and  $\bar{r}_0$  defines the trap geometry. This equation was generalized to stretched geometries, where  $\bar{r}_0^2 = r_0^2 + 2z_0^2$ . Setting  $\bar{r}_0 = r_0$  and dividing the right-hand side of Eq. (8) by 2 yields the expression for pure quadrupole field traps. The right-hand side of Eq. (8) can be multiplied by  $4/\pi$  to obtain the relation for a SIT.

The development of this expression yields some interesting observations. For example when the dipole excitation waveform is fixed, the ion mass at constant trapping voltage does not scale with the reciprocal of the trapping frequency squared. Ding et al. [2] bypassed this problem by phase locking the excitation and trapping frequencies thereby making  $m_{\text{ej}}$  proportional to  $\Omega^{-2}$ . Our expression permits the determination of the ejected mass for any experiment that varies the voltage, trapping frequency and excitation frequency or any combination thereof. This permits rapid mass calibration for any type of mass scan in an ion trap.

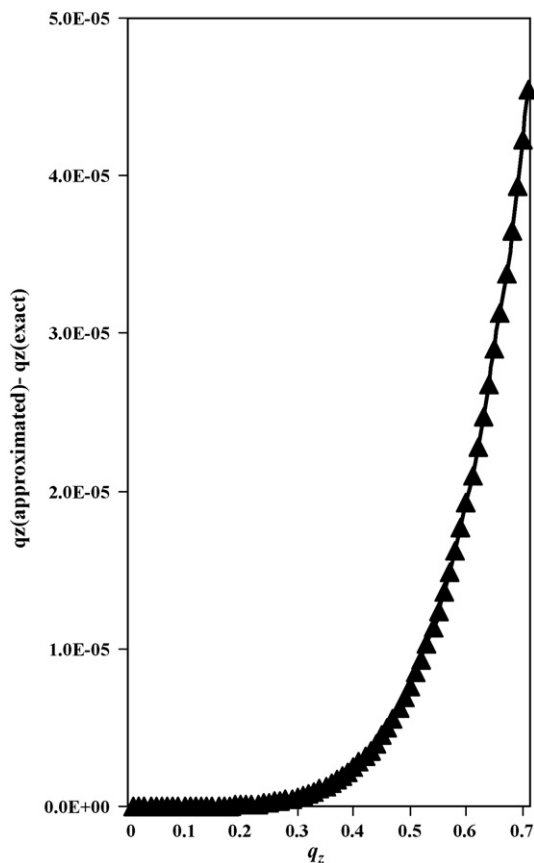


**Fig. 2.** A plot of the difference between our approximation of  $q_z$  and its exact value and a function of  $q_z$ . Values of  $q_z$  spanning the range of stable values were used with the exact expression derived by Ding et al. [3] (Eq. (3)) to calculate the secular frequencies of the ions over that range. These secular frequencies were then used with our approximation (Eq. (6)) to calculate  $q_z$ . The difference between the approximated and exact values is plotted as a function of  $q_z$ .

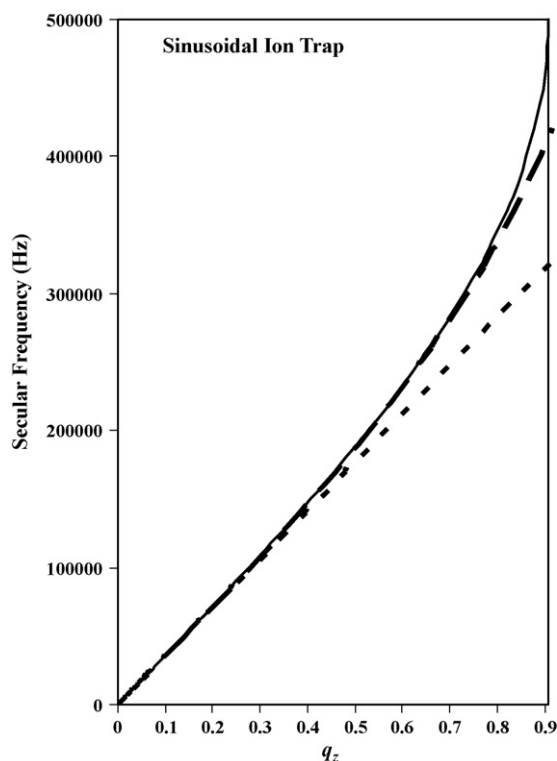


**Fig. 3.** A plot of the ion secular frequency in a SIT operated at a trapping frequency of 1000 kHz versus the Mathieu parameter,  $q_z$ , derived from Eq. (6) is shown as a solid black line. A plot of the ion secular frequency using the pseudo-potential well approximation (Eq. (1)) is depicted as a dotted line. The dashed line shows the results derived from Eq. (2) from Trevitt et al. [14].

### 3. Evaluation of the scanning methods

There are three different types of high resolution scanning methods in the literature. The first holds the trapping waveform constant and sweeps or steps the excitation frequency. This was the method applied by Goeringer et al. [9] to obtain a resolution of 45,000 using a SIT. We found it instructive to plot the log of the ion mass-to-charge ratio as a function of ion secular frequency for various values of the DIT trapping frequency,  $f = 250, 500, 750$  and 1000 kHz and  $\Omega = 2\pi f$  (see Fig. 4). For these plots,  $V = 750 V_{0-p}$  and  $r_0^2 = 0.000177 \text{ m}^{-2}$ . We also imposed the boundary conditions over which Eq. (7) is valid,  $0 \leq q_z \leq 0.7125$  for a DIT [2]. Each of the plots in Fig. 4 were truncated at the  $\beta_z = 1$  boundary that occurs at the first minimum in the function, where  $\Omega/2 = \omega_{\text{sec}}$ . Beyond

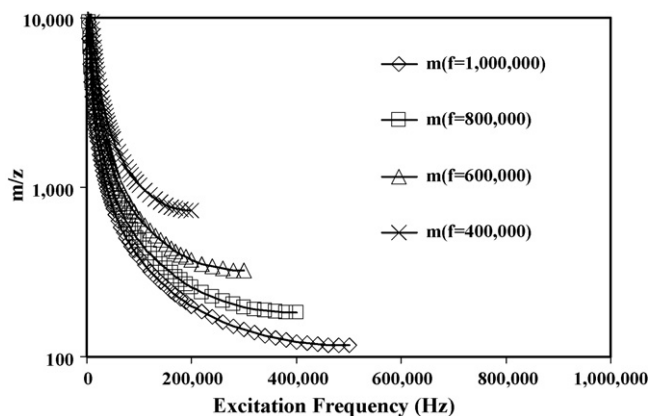


**Fig. 4.** A log plot of the mass-to-charge ratio ( $m/z$ ) versus excitation frequency for a range of constant trapping frequencies—1000, 750, 500, and 250 kHz.

that point the function is not valid. Because the derivative of the log of  $x$  is proportional to  $1/x$ , the slope of the log of the ejection mass is proportional to the reciprocal of the resolution,  $\Delta m/m$ . Log plots of the ejection mass as a function of frequency provide a convenient method for comparing differences in resolution. The highest resolution should be obtained when the slope of the function is the lowest. This occurs at the higher frequencies where the changes in the excitation frequency are largest between each nominal mass. Other studies [9,16] have also noted better resolution with increasing  $q_z$  suggesting that the contribution to the line width due to damping is smaller at higher ion oscillation frequencies and the variation of those frequencies with mass is greater. One of the studies revealed that resolution decreases in the vicinity of the boundary at  $\beta_z = 1$  because the simple harmonic motion model becomes less accurate as the amplitude at the fundamental frequency increases [9]. Presumably, the highest resolution will occur just short of where the boundary begins to affect the ions. It is evident that high resolution conditions exist over a limited range. However, that range can easily be adjusted up or down in mass by changing the trapping frequency as shown in Fig. 4. It is also noted that while the vertical position of the high resolution region with the lowest slope readily increases with decreasing trap frequency and the range of excitation frequencies where high resolution is achieved gets smaller. This is not really an issue. The frequency resolution should increase with decreasing frequency because as the period of the waveform gets longer while the jitter that defines the error in producing the wave should remain constant under ideal conditions. This suggests that high resolution in the ultrahigh mass range can be obtained with sufficient control of the applied waveforms.

The next resonant ejection method holds the excitation frequency waveform constant while sweeping or stepping the trapping conditions. In a SIT the trapping voltage is linearly swept, while in a DIT the frequency is stepped. The frequency control in a DIT can be so precise that the mass can be stepped linearly with time. In both the SIT and the DIT, changing the trap conditions changes the secular frequency of the ions while the excitation waveform remains constant. From the point of view of the ions, these two techniques are essentially equivalent—excluding the difference in the waveforms. We have plotted the log of the mass-to-charge ratio as a function of trapping frequency in Fig. 5 for excitation frequencies of 250, 200, 150 and 100 kHz at  $750 V_{0-p}$ . These plots are truncated on the left-hand side because the boundary conditions,  $0 \leq q_z \leq 0.7125$ , require that the trapping frequency be at least double the excitation frequency. Once again the flattest portion of the curve should provide the best resolution provided the excitation frequency is far enough from half of the trapping frequency so that

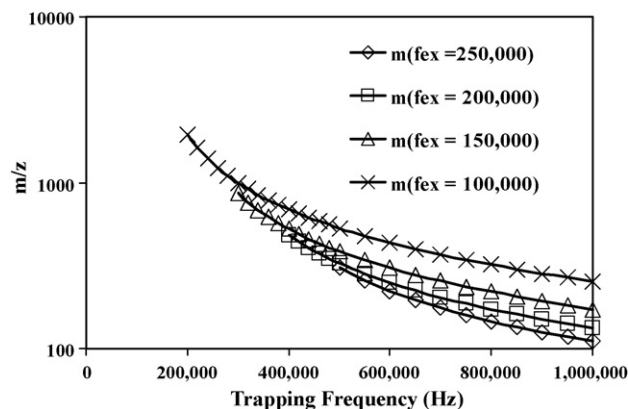


**Fig. 5.** A log plot of the mass-to-charge ratio ( $m/z$ ) versus trapping frequency for a range of constant excitation frequencies—100, 75, 50, and 25 kHz.



the ions are not excited by the boundary at  $\beta_z = 1$ . This mode can also be used to obtain high resolution in the ultrahigh mass range.

To complete the comparison, we plotted the log of the mass-to-charge ratio as a function of trapping frequency at constant voltage ( $V = 750 V_{0-p}$ ) under phase-locked conditions for values of  $\Omega/\omega_{ex}$  ranging from 3 to 8 in Fig. 6. The curves do not shift much for small changes in the integer values of  $\Omega/\omega_{ex}$ . The highest resolution should occur where the curves are the flattest toward higher trapping frequency and the resolution appears to increase with increasing  $\Omega/\omega_{ex}$ .

The log plots for each scanning method were plotted on the same scale so that direct comparisons could be made. Figs. 5 and 6 permit the comparison of the resolution for fixed excitation frequency and excitation frequency locked scanning of the trapping frequency. The slopes of the curves in the fixed excitation frequency plots are smaller at the higher trapping frequencies than the locked curves. This suggests that higher resolution should be achievable in fixed excitation frequency scanning mode. Comparison of Figs. 5 and 6 to Fig. 4 suggest that scanning the excitation frequency should provide better resolution than scanning the trapping frequency.

The results of our comparison of the scanning methods seem to be in contradiction to the results of Ding et al. [3] and Londry and March [17] who found that the frequency locked mode of scanning provides better resolution than the “unlocked” methods. We point out that our analysis does not consider the dynamics of the ejection process. We do not consider the effects of the relative phases of the excitation and trapping waveforms, higher order field perturbation, gas pressure, scanning direction and scanning speed on resolution. These factors have been covered extensively in the literature for SITs and their treatments are extendable to DITs. Furthermore, we do not consider the case where the duty cycles of the DIT waveforms were optimized. We merely suggest that, for a given step size of the waveform frequency, scanning the excitation waveform while holding the trapping waveform constant will result in the smallest mass step; however, this may not necessarily provide the best resolution. The dynamics of the ions before and during the ejection process have to be considered for a complete discussion of resolution.

The results in Figs. 4–6 are completely generalizable to SITs. However, commercial SITs operate with resonantly tuned rf circuits that scan by sweeping the trapping voltage. Scanning the trap frequency is not generally an option. However, that was never a concern because the ion mass is always a linear function of the trapping rf voltage no matter what excitation frequency is used. We illustrate that point in Fig. 7 by plotting the ion mass for a 1 MHz SIT as a function of trapping voltage for excitation frequencies of 500, 200, 100, 50 and 25 kHz. Before now, the slopes of these curves were

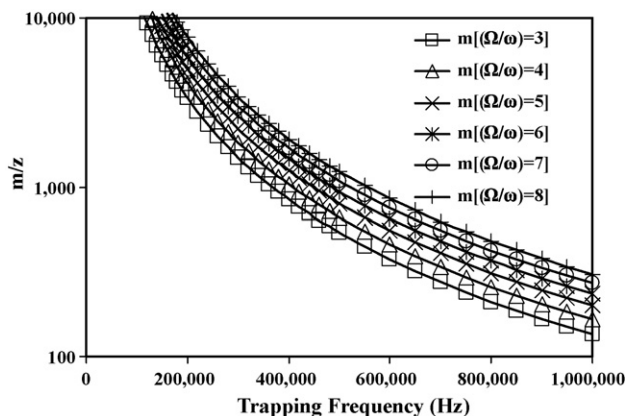


Fig. 6. A log plot of the mass-to-charge ratio ( $m/z$ ) versus trapping frequency for phase locked resonant ejection at  $(\Omega/\omega) = 3, 4, 5, 6, 7$  and  $8$ .

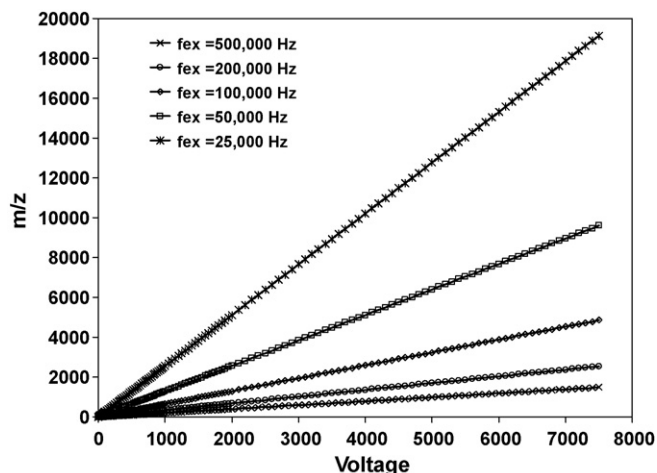
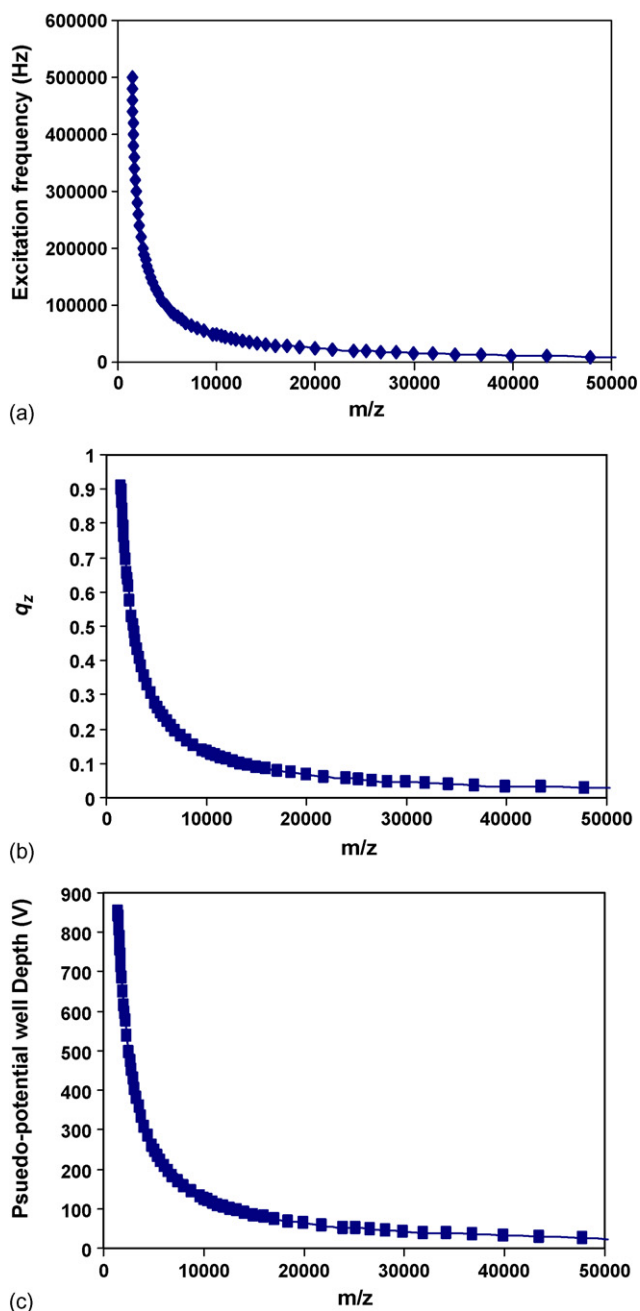


Fig. 7. A plot of the mass-to-charge ratio ( $m/z$ ) versus trapping voltage for excitation waveform frequencies,  $f_{ex} = 25, 50, 100, 200, 500$  kHz.

not easily predicted; however, that was never an issue because they could be determined with the measurement of a couple of known analytes. Whether or not the excitation waveform is phase locked has no effect on the rate of change of the ejection mass with trap voltage. Therefore, it will not affect the mass step resolution even though it has been shown to dramatically affect the ultimate mass resolution achieved [17]. Phase locking affects the dynamics of the ejection process not the mass step.

In a previous publication [18], we pushed resonant ejection to its limits in a 1 MHz SIT using the aerosol MALDI technique to produce ions inside the trap. Ions up to myoglobin ( $m/z = 16.9$  kDa) were produced and trapped. Trapping was successful because the trapping voltage was set to its maximum, at approximately  $7500 V_{0-p}$ , to maximize the pseudo-potential well depth during the MALDI process. The trapping potential was then lowered and an auxiliary potential was applied to the endcap electrodes at constant frequency and voltage during the rf voltage ramp. We found that the resolution degraded with increasing mass. Good signal and resolution were obtained up to approximately 3.5 kDa (insulin chain B) beyond which the quality of the data deteriorated rapidly. We suggested that the pseudo-potential well depth preceding and during ion ejection was the major factor that defined the resolution and the signal-to-noise ratio. Unfortunately, the rf voltage and therefore the pseudo-potential well depth had to be decreased in order to scan the masses out of the trap.

We could have maintained the rf voltage and scanned the ions out of the trap by sweeping or stepping the auxiliary potential frequency on the endcap electrodes if we had an easy way of calibrating the instrument. We now have that. This scanning method will markedly enhance the mass range of current commercial ion traps. To demonstrate this we have calculated the resonant excitation frequency as a function of mass for a  $7500 V_{0-p}$ , 1 MHz trapping potential in Fig. 8(a). The value of  $q_z$  as a function of  $m/z$  is plotted in Fig. 8(b). The pseudo-potential well depth as a function of  $m/z$  is plotted in Fig. 8(c). This assumes the pseudo-potential well approximation is accurate for all bound values of  $q_z$  where the well depth  $D = q_z V/8$ . However, it is well known that this approximation is only good up to  $q_z = 0.4$ . The truncation of the use of this approximation at or below  $q_z = 0.4$  was due to the inability to easily and reliably calculate  $q_z$ . That no longer is an issue. Therefore, the pseudo-potential well depth can be calculated beyond  $q_z = 0.4$  with the above expression and our calculation for  $q_z$ . The well depth in reality continues to increase after  $q_z = 0.4$  and then rapidly decreases to zero near the boundary at  $\beta_z = 1$  where the high frequency oscillations become dominant. Nonetheless, the behavior of the ions where the well



**Fig. 8.** A plot of (a) the excitation frequency, (b) the Mathieu parameter  $q_z$  and (c) pseudo-potential well depth versus the mass-to-charge ratio for a commercial 1 MHz SIT at maximum trapping voltage (7500  $V_{0-p}$ ).

depth is large is not an issue. Real problems with resolution and sensitivity occur when the well depth becomes too small. Our results suggest that the well depth is greater than 100 V at 10 kDa and is approximately 30 V at 40 kDa (see Fig. 8(c)). Our results from our aerosol MALDI suggest that good resolution should be achievable well past 10 kDa and could reach as high as 40 kDa or more. That represents a big improvement in mass range that could be extended even higher with a lower frequency ion trap.

#### 4. Conclusions

We have derived analytical expressions for the ejection mass from sinusoidal and square wave ion trap under any set of resonant ejection conditions for stable values of  $q_z$ . These expressions were then used to evaluate resonance scanning methods in terms of mass step resolution. Our results suggest that ion traps operate better at higher values of excitation frequency or  $q_z$ . In DITs, where mass scans are generally performed by stepping the trapping frequency, phase locked resonance scanning yields lower mass step resolution than fixing the excitation waveform. However, scanning the excitation waveform, while fixing the trapping waveform, produced even better mass step resolution. We have also extended our analysis to SITs and showed that we are now able to calculate the slope of the ejection mass versus trap voltage. Our extension of the analysis to SITs suggests a viable method for extending the operational mass range for commercial ion traps. Our analysis suggests that a 1 MHz trap could yield well resolved mass spectra up to 10 kDa and higher by maximizing the trapping voltage and scanning the excitation frequency. The question remaining is, where does the resolution break down and why? We further suggest that lower frequency traps should yield a much higher mass range. An improvement in mass range and resolution of ion traps opens new possibilities for biological mass analysis especially for top down proteomics.

#### Acknowledgement

This research was paid for by maturation funding from UT-Battelle, LLC under contract no. DE-AC05-00OR22725 with Oak Ridge National Laboratory, managed and operated by UT-Battelle, LLC.

#### References

- [1] L. Ding, S. Kumashiro, *Rapid Communications Mass Spectrometry* 20 (2006) 3.
- [2] L. Ding, M. Sudakov, F.L. Brancia, R. Giles, S. Kumashiro, *Journal of Mass Spectrometry* 39 (2004) 471.
- [3] L. Ding, M. Sudakov, S. Kumashiro, *International Journal of Mass Spectrometry* 221 (2002) 117.
- [4] J.A. Richards, *International Journal of Mass Spectrometry and Ion Processes* 24 (1977) 219.
- [5] J.A. Richards, R.M. Huey, J. Hiller, *International Journal of Mass Spectrometry and Ion Physics* 12 (1973) 317.
- [6] L. Cordesses, *Direct Digital Synthesis: A Tool for Periodic Wave Generation (Part 1)*, *IEEE Signal Processing Magazine* July 2004, pp. 50–54.
- [7] L. Cordesses, *Direct Digital Synthesis: A Tool for Periodic Wave Generation (Part 2)*, *IEEE Signal Processing Magazine* September 2004, pp. 110–117.
- [8] V.F. Kroupa, *Direct Digital Frequency Synthesizers*, Institute of Electrical and Electronics Engineers, New York, 1999.
- [9] D.E. Goeringer, W.B. Whitten, J.M. Ramsey, S.A. McLuckey, G.L. Glish, *Analytical Chemistry* 64 (1992) 1434.
- [10] P.H. Dawson, *Quadrupole Mass Spectrometry and Its Applications*, AIP Press, Woodbury, NY, 1995, p. 65.
- [11] R.E. March, *Journal of Mass Spectrometry* 32 (1997) 351.
- [12] R.E. March, J.F.J. Todd, *Practical Aspects of Ion Trap Mass Spectrometry: Fundamentals*, vol. 1, CRC Press, Boca Raton, FL, 1995, p. 83.
- [13] H.G. Dehmelt, *Advances in Atomic and Molecular Physics* 3 (1967) 53.
- [14] A.J. Trevitt, P.J. Wearne, E.J. Bieske, *International Journal of Mass Spectrometry* 262 (2007) 241.
- [15] N.W. McLachlan, *Theory and Application of Mathieu Functions*, New York, 1962.
- [16] A. Moradian, D.J. Douglas, *Journal of the American Society for Mass Spectrometry* 19 (2008) 270.
- [17] F.A. Londry, R.E. March, *International Journal of Mass Spectrometry and Ion Processes* 144 (1995) 87.
- [18] W.A. Harris, P.T.A. Reilly, W.B. Whitten, *International Journal of Mass Spectrometry* 258 (2006) 113.